NASA/TM-1999-209352
ARL-TR-1978

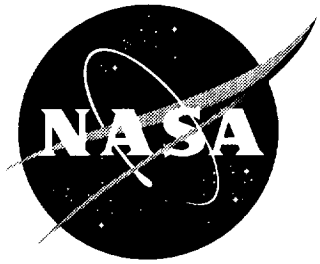

Advanced Modeling Strategies for the Analysis of Tile-Reinforced Composite Armor

Carlos G. Dávila and Tzi-Kang Chen
U.S. Army Research Laboratory
Vehicle Technology Directorate
Langley Research Center, Hampton, Virginia

National Aeronautics and
Space Administration

Langley Research Center
Hampton, Virginia 23681-2199

July 1999

The use of trademarks or names of manufacturers in the report is for accurate reporting and does not constitute an official endorsement, either expressed or implied, of such products or manufacturers by the National Aeronautics and Space Administration or the U.S. Army.

Available from:

NASA Center for AeroSpace Information (CASI)
7121 Standard Drive
Hanover, MD 21076-1320
(301) 621-0390

National Technical Information Service (NTIS)
5285 Port Royal Road
Springfield, VA 22161-2171
(703) 605-6000

ADVANCED MODELING STRATEGIES FOR THE ANALYSIS OF TILE-REINFORCED COMPOSITE ARMOR

C. G. DÁVILA and TZI-KANG CHEN

Army Research Laboratory, Vehicle Technology Center
NASA Langley Research Center, Hampton, VA 23681

Abstract.

A detailed investigation of the deformation mechanisms in tile-reinforced armored components was conducted to develop the most efficient modeling strategies for the structural analysis of large components of the Composite Armored Vehicle. The limitations of conventional finite elements with respect to the analysis of tile-reinforced structures were examined, and two complementary optimal modeling strategies were developed. These strategies are element layering and the use of a tile-adhesive superelement. *Element layering* is a technique that uses stacks of shear deformable shell elements to obtain the proper transverse shear distributions through the thickness of the laminate. The *tile-adhesive superelement* consists of a statically condensed substructure model designed to take advantage of periodicity in tile placement patterns to eliminate numerical redundancies in the analysis. Both approaches can be used simultaneously to create unusually efficient models that accurately predict the global response by incorporating the correct local deformation mechanisms.

Key words: composite armor, tile-reinforced sandwich structure, element layering, superelements.

1. Introduction

Virtually every aerospace company and many land-vehicle manufacturers are developing products made with fiber-reinforced composite materials. In the last thirty years, the use of composite materials has progressed through several stages. The early stages consisted of replacing a metallic component with a similarly designed composite part. The current stage of composite material usage is the all-composite vehicle. This long-held vision is now possible with the development of new fundamental insight into the mechanics issues of composite structures along with new analytical and computational tools.

The Composite Armored Vehicle (CAV) is an Advanced Technology Demonstrator designed and manufactured in 1998 by United Defense, L.P. (UDLP), of San Jose, CA. The vehicle, which is shown in Fig. 1, was designed to demonstrate a 33% reduction in the combined weight of the armor and the structure compared to the weight of an all-metallic baseline vehicle with equivalent protection. The upper hull of the vehicle consists of a sandwich of ceramic tiles bonded between a thick glass-epoxy inner hull and a thinner outer hull. To isolate the tiles from the inner hull and to improve damage tolerance, a rubber layer is built into the laminate. The ceramic tiles are bonded to each other and to the surrounding materials with a tough and highly compliant adhesive that limits the propagation of damage to the surrounding tiles.

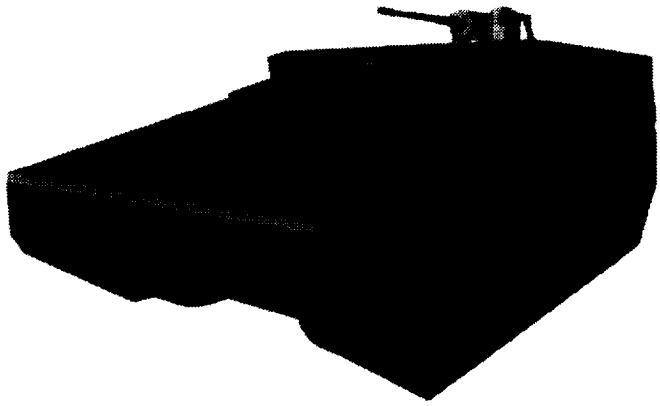

Figure 1. Composite Armored Vehicle Advanced Technology Demonstrator.

The proper balance between structural and ballistic performances was optimized in the CAV design by tailoring the interaction between the rubber, ceramic tile, glass-epoxy, and adhesive to achieve a design that integrates structure and armor. To the analyst, however, the juxtaposition of materials with very different stiffnesses poses computational difficulties unlike those of typical composite structures. It was found that standard finite element techniques provide inaccurate results for this type of construction.[1]

In the following section, the response characteristics of the CAV upper hull and the corresponding limitations of shell elements used in finite element analysis are discussed. To address these limitations, two complementary analysis techniques are proposed. The technique referred to herein as element layering improves the global and local response prediction accuracy of conventional shell elements by stacking layers of shell elements. The computational efficiency can be further improved by taking advantage of the periodicity in the CAV construction by using superelements. The second technique is based on superelements, which simplifies the task of modeling, virtually eliminates the time required to assemble the stiffness matrices, and significantly reduces the analysis solution time.

2. Response Characteristics of the CAV Upper Hull

The core of the CAV upper hull consists of 10.2-by-10.2 cm-square ceramic armor tiles. The CAV upper hull achieves its ballistic performance through the complex interaction of brittle ceramic tiles, tough S2-glass/epoxy plies, and low modulus rubber and adhesive materials. Large differences in moduli and size occur in both the thickness and the in-plane directions, as shown in Fig. 2. Consequently, the strain distributions in this structure are quite different from what might be expected in an isotropic structure. In particular, two aspects of the local deformation of tile-reinforced laminates pose challenges to the analysis. The first difficulty is due to the variation of properties in the thickness direction; the other is due to the variation of the in-plane properties.

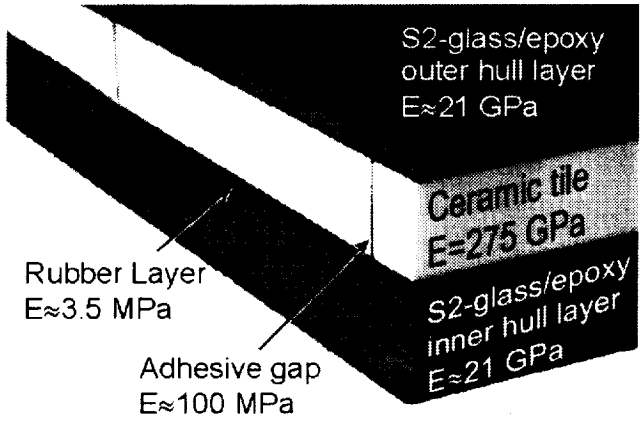

Figure 2. Photograph of the edge of a CAV upper hull specimen. Approximate values of Young's moduli illustrate the large variations in properties between adjacent materials.

The deformation of a three-dimensional model of a CAV beam subjected to three-point bending is shown in Fig. 3. It can be observed that the beam deforms less like a monolithic structure and more like two loosely coupled laminates, one on top of the other. The softness of the rubber mat allows some relative motion to occur between the upper and lower portions of the laminate. This relative motion invalidates the assumptions used for conventional shell finite elements.

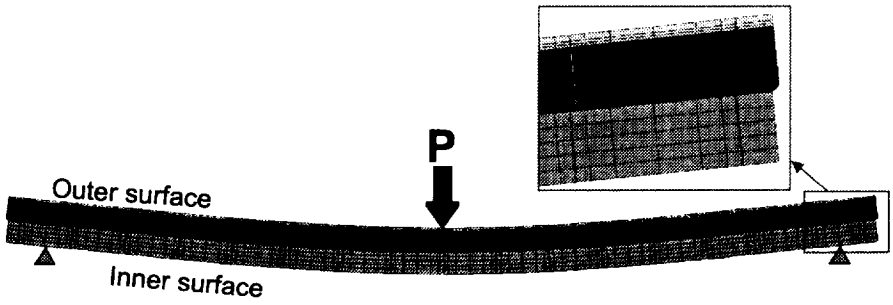

Figure 3. Three-dimensional model of a CAV beam subjected three-point bending. Free edges of beam display transverse shearing of rubber layer.

In addition to the changes in material properties through the thickness, there is also an in-plane periodicity due to the adhesive-filled gaps between tiles. The tiles are aligned in a pattern consisting of staggered rows. The bondline is orders of magnitude smaller than the length of a tile, yet it elongates more than a tile, as can be seen from the plane strain model shown in Fig. 4. The periodicity in the deformations is most apparent in the distribution of strains along the surfaces of the laminate. The axial strains shown in Fig. 5 correspond to the outer and inner surfaces of the beam shown in Fig. 3 subjected to three-point bending loads. The surface strains are the strains that can be measured with strain gages bonded to the surfaces of the specimen. The outer surface strains are highly periodic, with large local increases in strain at the location of the tile gaps. The strains on the inner surface are smooth because the thick glass-epoxy inner hull and the rubber layer even out the variations. The presence of such large concentrated bending, shearing and

extensional deformations at the adhesive gaps requires the use of extremely small and detailed finite element meshes to represent the local response characteristics accurately.

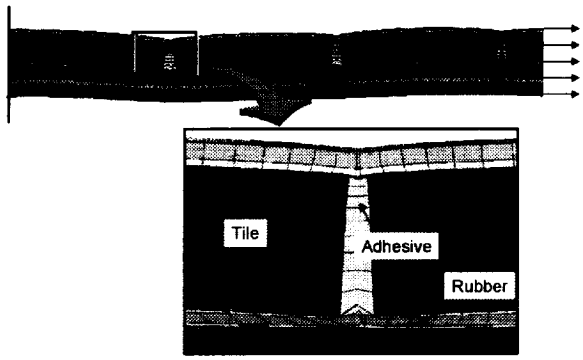

Figure 4. Plane strain analysis of sandwich beam in tension. High compliance of the small adhesive bondline results in a relatively large opening of the gap.

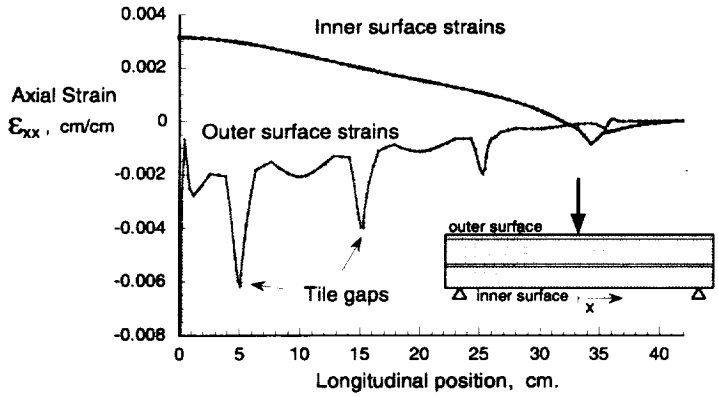

Figure 5. Strains on the surfaces of a beam subjected to three-point bending. The strains on the outer surface have local increases at the gaps between tiles; those on the inner surface are smooth.

While three-dimensional solid models are often the only means of predicting complex stress fields, they are currently so computationally expensive that they are impractical for the analysis of anything other than small and relatively simple components. The methods presented in the present paper do not add fidelity to the solution compared to a detailed three-dimensional model. However, element-layering and tile-adhesive superelements predict nearly or exactly the same results as an equivalently meshed solid model at a fraction of the computational cost of the solid model.

3. Analysis of CAV Upper Hull Laminates with Shell Elements

Most finite element analyses of thick composite structures rely on so-called thick-shell elements. These computationally efficient elements are based on the Mindlin-Reissner (MR) kinematic assumptions that state that the normal to the shell remains straight and does not elongate. The MR assumptions imply that the transverse shear in the shell is constant through the thickness, and this theory is referred to as a First Order

Transverse Shear Deformation Theory (FSDT). One inconsistency in this theory is that the constant transverse shear does not satisfy the traction-free boundary conditions at the top and bottom faces of a laminate. This inconsistency is usually offset by applying a shear correction factor (SCF) to the transverse shear stiffnesses. For isotropic materials, where the transverse shear distribution due to a static load is exactly parabolic, the SCF is 5/6. Whitney[2] and others have proposed methods for computing the SCF for non-isotropic materials, and it may seem reasonable to expect that it is possible to compute a SCF for the CAV laminate. However, numerical simulations and tests show that it is not possible to compute a single SCF for all CAV analyses. For example, the results of shell analyses of a plate subjected to three-point-bending loads are shown in Fig. 6 for various SCFs. The stiffness of the plate is plotted as a function of the SCF. A SCF of 5/6 results in an overly stiff response that corresponds to the response of a monolithic plate. The SCF computed using Whitney's method is only 0.04. This low value causes an overly compliant deformation that almost corresponds to a beam with pure shear deformation (no bending) with near zero slope outboard of the supports. A comparison of the analytical results with experimental results suggests that a SCF of 0.1 corresponds to the proper mid-span deflection, but it can be shown that this number varies with specimen length.[1] In other words, the unusual through-the-thickness strain distributions in laminates with embedded tiles cannot be represented by conventional shell elements, and conventional SCFs do not properly account for the concentration of transverse shear in the rubber layer without unbalancing the ratio of shearing and bending energies.

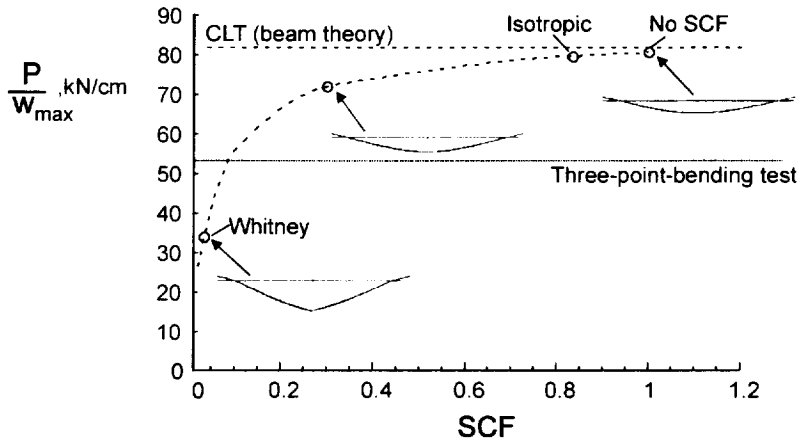

Figure 6. Effect of shear correction factor on the global stiffness and bending mode of a 33-inch-long by 16-inch-wide plate subjected to three-point bending loads, with a 27-inch-long support span.

3.1 Element Layering for Higher-Order Transverse Deformation

Shell elements of high order in transverse shear are becoming relatively common in research codes. Averill's shell elements[3] with high-order zig-zag sublaminate approximations, for instance, can even simulate delaminations by using plies of nearly zero material stiffness. However, higher-order elements usually possess a large number of degrees of freedom per node, which renders their implementation into commercial finite element codes rather complex. Furthermore, the present study involves the

cooperative analysis efforts and computational facilities of several vehicle manufacturers and government laboratories, so a solution to the lack of accuracy of shell elements had to be compatible with typical commercial finite element codes. The solution adopted in the present paper consists of the method of *element layering*, a technique that has been previously applied to the computation of fracture parameters in skin-stiffener debond problems.[4] Element layering is designed to provide the needed higher order in transverse deformations. The method simply consists of modeling the laminated composite shell with more than one thick-shell element through the thickness, where each element layer comprises a sublaminate of similar material properties. The CAV upper hull laminate is layered into four element layers: 1) a glass-epoxy inner-hull layer; 2) a rubber layer; 3) a tile layer; and 4) an outer glass-epoxy layer. The layers are tied together in the model with multi-point constraint (MPC) equations that enforce displacement compatibility at the layer interfaces. Continuity requires that the displacements on both sides of the common interface between two regions be equal. MPC's do not model the stiffness of the adhesive gap, they model the compatibility of displacements at the boundary surface separating two arbitrary regions. Using the Mindlin-Reissner kinematic equations of FSDT, the compatibility equations at an interface are

$$\begin{aligned} u_l + \tfrac{t_l}{2}\theta_l^y &= u_u - \tfrac{t_u}{2}\theta_u^y \\ v_l - \tfrac{t_l}{2}\theta_l^x &= v_u + \tfrac{t_u}{2}\theta_u^x \\ w_l &= w_u \end{aligned} \tag{1}$$

where u_u and u_l are the displacements of the layers above and below the interface, and θ_u and θ_l are the rotations of the layers above and below the interface, respectively, as shown in Fig. 7.

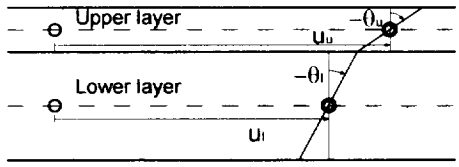

Figure 7. Multi-Point Constraints consistant with the Mindlin-Reissner kinematics of FSDT are used to enforce displacement continuity at the interface between two bonded layers. The displacements at the interface are functions of the translation component, u, the rotation, θ, and the thickness of the layer, t.

Most finite element codes require the separation of the degrees of freedom into dependent and independent degrees of freedom u_i and u_d, respectively. The separation is achieved by partitioning the constraint equation matrix as

$$\begin{bmatrix} M_i & M_d \end{bmatrix} \begin{Bmatrix} u_i \\ u_d \end{Bmatrix} = \begin{Bmatrix} 0 \\ 0 \end{Bmatrix} \Rightarrow u_d = -M_d^{-1} M_i u_i \tag{2}$$

For instance, after separation of the dependent and independent degrees of freedom, the x-direction MPC's for a four-layer model can be written as

$$\begin{Bmatrix} \frac{t_2}{2}\theta_2^y \\ \frac{t_3}{2}\theta_3^y \\ \frac{t_4}{2}\theta_4^y \end{Bmatrix}_{dependent} = \begin{bmatrix} -1 & 1 & 0 & 0 & -1 \\ 1 & -2 & 1 & 0 & 1 \\ -1 & 2 & -2 & 1 & -1 \end{bmatrix} \begin{Bmatrix} u_1 \\ u_2 \\ u_3 \\ u_4 \\ \frac{t_1}{2}\theta_1^y \end{Bmatrix}_{independent} \tag{3}$$

Element layering introduces two additional degrees of freedom per node for each additional layer. If a conventional model has six degrees of freedom per node, a two-layer model has eight, and a four-layer model has twelve. Note that element layering does not require SCFs since the transverse shear distribution is nearly constant in each layer. This observation is especially true for the thin rubber layer near the center of the CAV laminate.

A comparison between the results for a layered model and for a three-dimensional *(3D)* model in bending is shown in Fig. 8. The left portion of the figure shows three four-layer shell models of an 84-cm-long plate with varying support spans, L_s. The right portion of the figure shows the corresponding *3D* model. The agreement between the two types of models is excellent for all three support spans.

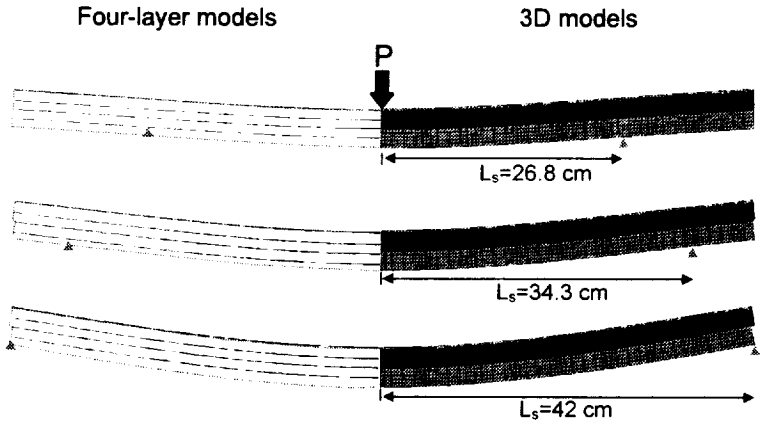

Figure 8. Simulated beam in bending. Results from four-layer models indicate excellent agreement with three-dimensional models at a small fraction of the computational cost.

A composite armored vehicle is designed with a number of structural features that may restrain transverse shearing at the free edges of the laminates. Unlike a simple three-point-bending test, few edges of the vehicle are unrestrained. The components are typically bonded and bolted together, and they possess built-in corners. Even the large circular turret opening on the roof is reinforced with a steel and aluminum turret bearing. In a conventional shell-based finite element analysis, there is no mechanism for applying end "cap" restraints that prevent shear deformations at the ends. In element-layered and *3D* models, there is sufficient through-the-thickness kinematic freedom to apply end-cap restraints. Analysis shows that an 84-cm-long CAV panel with end-cap restraints subjected to three-point bending is 85% stiffer than the same panel without end-cap restraints.[1]

The graphs shown in Fig. 9 summarize the results of three modeling techniques applied to a panel subjected to three-point bending loads with varying support spans. The

L1 models consist of conventional, single-layer shell models with a SCF of 0.1 or 0.3. End-cap restraints cannot be applied to *L1* models. The *L4* models consist of four-layer shell models with and without end-cap restraints. The *3D* models refer to three-dimensional models with and without end-cap restraints. The results show the normalized stiffness of the plate as a function of support span length. The results are normalized by the deflection from beam theory, $PL^3/48EI^*$, where EI^* is the "equivalent" flexural rigidity of this laminate. The agreement between the results for the *L4* and *3D* models is excellent, as indicated by the correlation between results in the figure. The range between the results for the models with and without end-cap restraints indicates the uncertainty of the degree of restraint that may be present at any reinforced edge of the vehicle.

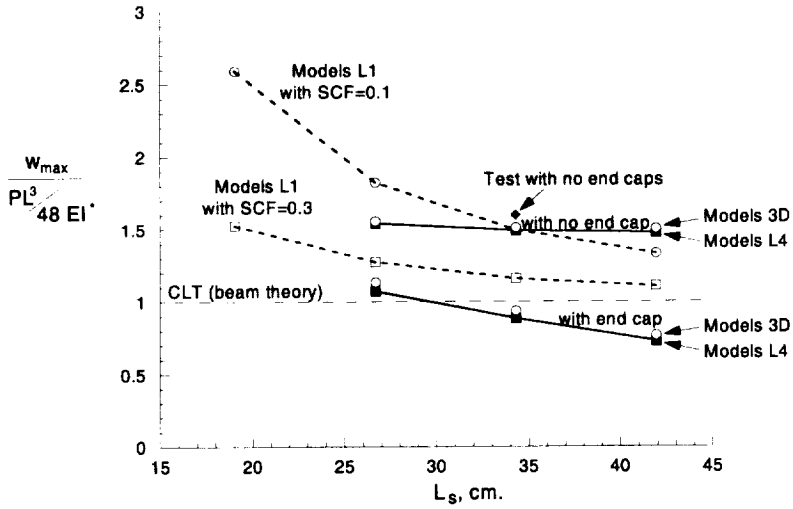

Figure 9. Normalized plate stiffness as a function of support span half-length. L1 represents a single-layer model and L4 represents a four-layer model.

To improve on the usefulness of the method, the element layering modeling procedure was automated to transform conventional shell models into multi-layered models. A FORTRAN program was developed to read in the information defining the nodes, element connectivities and section properties of a shell model, and to create automatically the new node locations, elements, section properties and MPCs of the corresponding layered model. Decisions such as the number of layers or thicknesses of each layer are made by the program based on the section properties of the elements in the original model. An example of a multi-layered half-model of the test specimen of the rear section of the CAV is shown in Fig. 10. The results of the analysis conducted with this model and the correlation with experiment are presented in Reference 5.

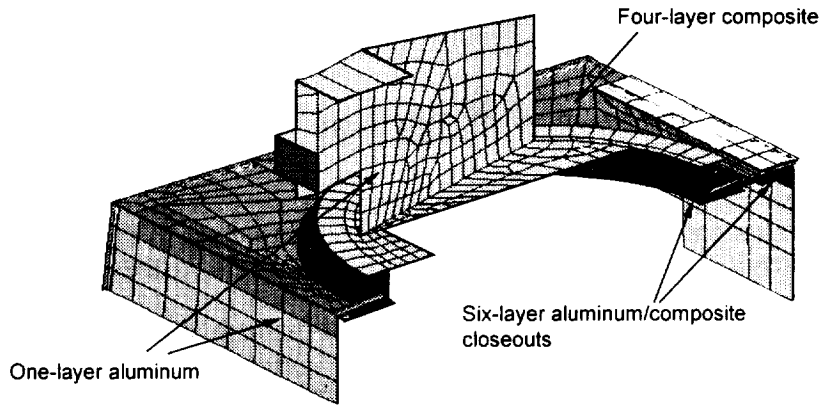

Figure 10. Multi-layered half-model of the rear section of the CAV. Metallic components are modeled with one element layer. Composite sections are modeled with four or six element layers.

4. Substructuring of Periodic Structures

The basic concept of substructuring consists of separating a model into parts, and eliminating all degrees of freedom except for those needed to connect the parts to the rest of the model. A reduced part appears in the model as a "superelement:" a collection of nodes and degrees of freedom connected by the superelement's stiffness and mass matrices. The reduced stiffness matrix is easily derived by partitioning the matrix of the substructure into the terms that multiply the retained degrees of freedom, u_r, and those that multiply the condensed (eliminated) degrees of freedom, u_c, as follows:

$$\begin{bmatrix} K_{cc} & K_{cr} \\ K_{rc} & K_{rr} \end{bmatrix} \begin{Bmatrix} u_c \\ u_r \end{Bmatrix} = \begin{Bmatrix} P_c \\ P_r \end{Bmatrix} \tag{4}$$

From the first equation, u_c can be extracted in terms of the retained degrees of freedom, u_r

$$u_c = K_{cc}^{-1}\left(P_c - K_{cr}u_r\right) \tag{5}$$

Substituting into the second line of Eq. 4 gives

$$K_{rc}K_{cc}^{-1}\left(P_c - K_{cr}u_r\right) + K_{rr}u_r = P_r \tag{6}$$

Rearranging the terms in Eq. 6 gives the condensed stiffness K^*

$$K^*u_r = P^* \quad \text{where} \quad \begin{cases} K^* = K_{rr} - K_{rc}K_{cc}^{-1}K_{cr} \\ P^* = P_r - K_{rc}K_{cc}^{-1}P_c \end{cases} \tag{7}$$

Substructuring introduces no additional approximation in static analysis; the superelement is an exact representation of the linear, static behavior of its members. However, the formation of the matrix K^* and the reduced load vector P^* are obtained at a computational cost equivalent to that of performing a Gaussian elimination of the degrees of freedom u_c from the full model's assembled stiffness matrix. In other words, no benefit is achieved from static condensation unless the superelement can be re-used in subsequent analyses or substructures.

Once the system's solution has been obtained, it is possible to recover the internal response of the superelement, provided that all terms in Eq. 5 are saved in the solution database.[6]

Superelements offer a number of advantages, some of which are important for CAV analyses, such as:

- System matrices (stiffness, mass) are small as a result of condensation. Only the superelement's retained degrees of freedom are used in the analysis.
- Duplication in the formation of the substructure's stiffness is eliminated when the same superelement is re-used.
- Superelement library files allow analysts to share superelements. In large design projects, large groups of engineers must often conduct analyses using the same substructures. Superelement library files provide a straightforward and simple way of sharing structural information.
- The task of modeling can be simplified by including intricate details inside the superelement. For instance, the small adhesive gap around a ceramic tile does not need to be modeled when using superelements.

The following list itemizes some of the main limitations imposed by the use of superelements

- Superelements are linear or a linear perturbation about a nonlinear state. In a nonlinear analysis, the stiffness is a function of the accumulated displacements, which vary from element to element. Therefore, even identical superelements no longer have the same stiffness matrix.
- Dynamic solutions are approximate: the static modes obtained by a reduced set of retained nodes may not fully represent the dynamic response. Methods that are used to improve the accuracy of superelements in dynamic analyses include Guyan reduction and mode augmentation procedures.[7] Dynamic solutions are not considered in this paper.
- The large number of degrees of freedom of a single superelement causes a large bandwidth, and highly populated matrices that can mitigate some of the computational advantages of superelements. Judicious selection of the size and number of superelements can increase computational performance.
- There is no pre-processor support for the creation of superelement models.

4.1 Superelement Models and Analyses of the CAV Upper Hull

The capabilities of superelement models and analyses in commercially available codes were studied in the course of this investigation. Because of its usage simplicity, its computational efficiency, and its suitability to CAV upper hull analyses, ABAQUS was selected for the present study (See Ref. 8).

Superelements are used in ABAQUS in much the same way as any other element. This procedure requires that the connectivity of the superelement be specified in the sequence in which the superelement was defined. Unfortunately, there is no graphical pre-processor that currently supports superelements, and establishing the superelement connectivities for a complex model without pre-processor support is impractical. In particular, to create a superelement model, a pre-processor must at least be able to: i) represent a superelement; ii) clone a superelement and position the image in the model with specified translations and rotations; and iii) export the superelements in the form of the appropriate finite element input files. The absence of these necessary features was overcome in MSC/PATRAN[9] with the use of *masterelements* and a custom PATRAN-to-ABAQUS translator.[8, 10, 11] Masterelements are nothing more than triangular and bar

elements arranged in a pattern that simulates a superelement. The triangular elements connect all the retained nodes along the periphery of the superelement, as illustrated in Fig. 11. The specialized translator determines the connectivity of a superelement by grouping and sorting all the nodes belonging to the same superelement, and exports the results in the form of an ABAQUS input deck.

The most efficient method of working with superelements is to pre-define libraries of compatible elements that can be reused in similar analyses. For instance, the present study is based on three libraries of elements: *L4.R3* (Fig. 12), *L4.R8*, and *3D.R3* (Fig. 13) (See Refs. 9, 11, and 12). The letter *L* indicates a superelement based on element layering, followed by the number of layers used. The notation *3D* indicates a superelement based on solid continuum elements. The number following the letter *R* indicates the level of mesh refinement. The lowest level of mesh refinement, R3, uses three elements along the side of one quarter of the tile, while R8 uses eight. Each of the three libraries is composed of three superelements: a full tile with half of the surrounding adhesive gap, a half tile, and a quarter tile. For the user's modeling convenience, PATRAN templates are provided for each of the superelement libraries.

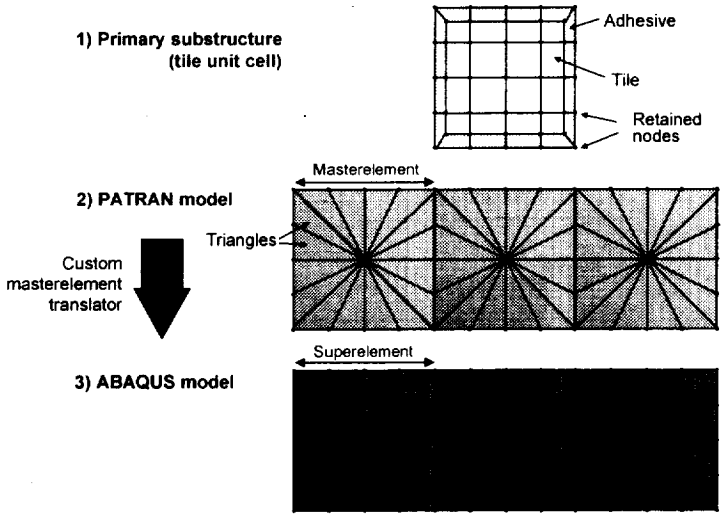

Figure 11. Triangles and bars are used to represent and clone superelements using PATRAN. A specialized translator sorts the nodes and writes the corresponding ABAQUS input file.

The element-layered libraries L4.R3 and L4.R8 are among the most computationally effective meshes that can be used to predict the response of tile-reinforced laminates. They derive their efficiency from the use of element layering with four layers of shear deformable 4-node quadrilateral ABAQUS shell elements (S4R) tied together with multi-point constraints. While these constraints can be difficult to write, they are internal to the superelements. Therefore, the constraints are totally invisible to the user of pre-defined superelement libraries.

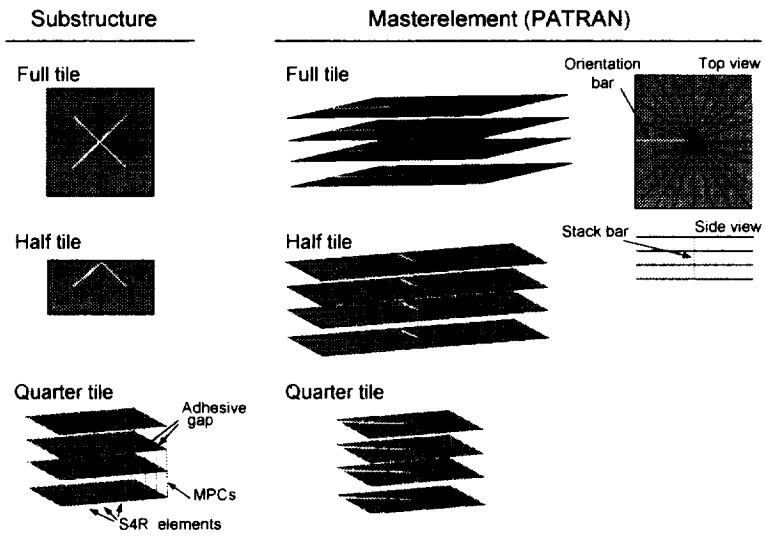

Figure 12. Superelement library L4.R3 is composed of quarter-tile, half-tile, and full-tile superelements. The corresponding PATRAN template has masterelements corresponding to each of these three superelements.

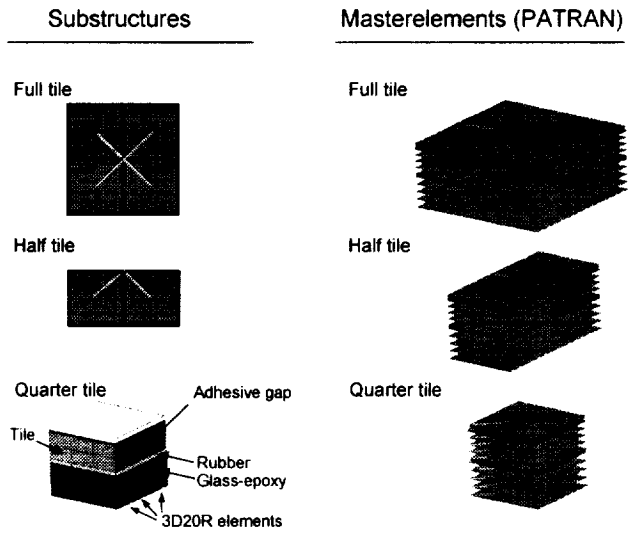

Figure 13. Superelement library 3D.R3 uses three-dimensional elements. The masterelements, however, still use triangles to represent the superelements in PATRAN.

4.1.1 Element-Layered Benchmark Analysis

Comparative analyses of the models shown in Fig. 14 were performed using standard elements and using superelements. Both models are based on element layering and their mesh refinement is the same. The panel dimensions are 4 tiles by 6 tiles, and the tile placement pattern is shown in Fig. 14. The applied load is 100 kN. The complexity of this benchmark problem was selected based on the computational cost of the standard model. The mesh refinement is relatively low, with elements in the gap region possessing

aspect ratios as high as 50-to-1. A more refined mesh, a larger panel, or a three-dimensional model would have resulted in an impractically large conventional model. The standard model uses 15,885 multi-point constraint equations (MPCs). The MPCs in the superelement model are internal to the superelement and, therefore, invisible to the user.

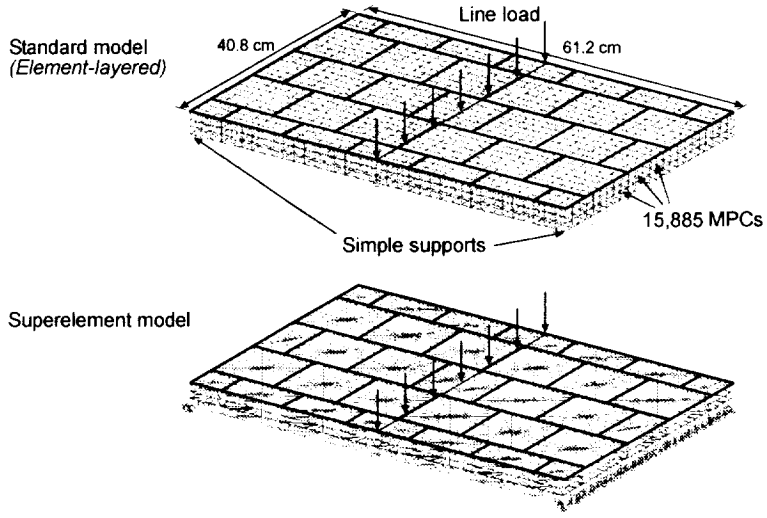

Figure 14. Comparative analyses of CAV-type composite armored plate subjected to three-point bending.

The results of the comparative study are shown in Table 1. As expected, the results for both analyses are identical. However, the superelement solution was obtained in 1/12th of the time needed for the reference solution. The reduction in solution time is not only the result of a reduced number of equations, but is also due to the reduction in the CPU time required to form and assemble the problem's stiffness matrix. When using superelements, the stiffness matrices are stored in solution database libraries, and do not need to be re-formed.

Another large difference between the two analyses is the total file size used by ABAQUS. The standard analysis uses 3,500 times more disk space because the problem is too big to fit into the memory of the workstation used for the analysis. Therefore, ABAQUS needs a swap file to solve the system of equations.

Table 1. Comparison of analysis using conventional elements and superelements.

	Standard Model	**Superelement Model**
Maximum deflection, cm.	1.11	1.11
Number of nodes	6,068	1,664
Number of equations	36,408	6,135
RMS wavefront	932	813
Total File size, MB	354	0.1
CPU model definition, sec.	374	14
Solution, sec.	303	43
TOTAL CPU time, sec.	677	57

4.1.2 CAV Analyses and Post-processing Examples

A comparison of the results for an 84-cm-long, 40.6-cm-wide panel subjected to three-point bending loads using three superelement libraries is shown in Table 2. The applied load is 100 kN, and the span between supports is 68.6 cm. The results indicate that the model using element library L4.R3 is only 1.5% stiffer than the model with element library L4.R8, even though a considerably less refined mesh was used. The deflections obtained from the element-layered models are approximately 25% larger than those for the model using the 3D library 3D.R3. This difference is due more to differences in modeling technique and properties, than to a more converged mesh.

Table 2. Comparison of results: plate subjected to three-point bending.

	L4.R3 Library	L4.R8 Library	3D.R3 Library
Degrees of freedom	8,597	41,827	16,973
RMS wavefront	2,217	6,198	2,922
Maximum deflection, cm.	1.48	1.51	1.99
CPU time, sec.	280	1,756	1,093

The ABAQUS/Post graphical post-processor works well with models using superelements based on element layering or solid elements. The results shown in Fig. 15 correspond to an analysis illustrating the use of library 3D.R3 to obtain detailed results from within selected superelements. The figure consists of a top-level (level-0) deformation plot superposed on lower-level plots of the strain distribution inside two highly stressed superelements. The results of this analysis would be the same as those of an identically refined model composed exclusively of three-dimensional elements. However, a direct comparison in solution time between the two models could not be completed due to the intractably large computational size of the conventional three-dimensional analysis.

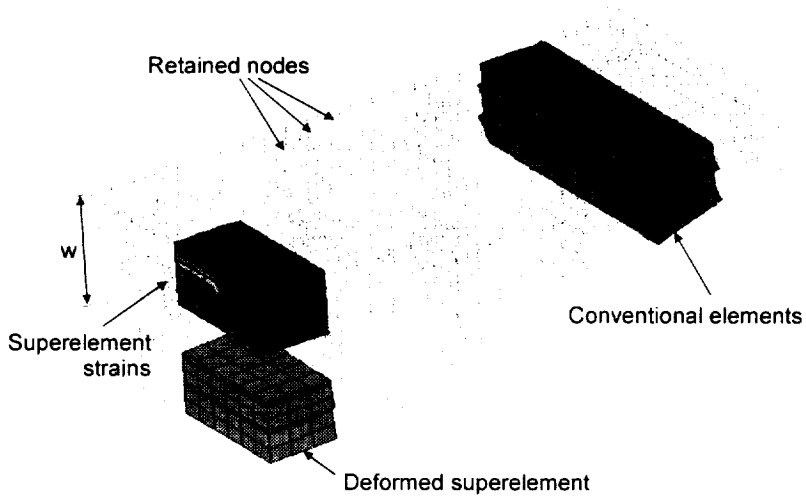

Figure 15. Results of analysis based on superelement library 3D.R3. Deformation and strains are shown for selected superelements. Retained nodes outline the superelements that have not been post-processed.

5. Concluding Remarks

An analytical study based on three-dimensional elements was conducted to determine the response characteristics of tile-reinforced composite armor components. The role of transverse shearing deformation in the rubber layer and the local shearing-bending deformations of the tile adhesive joints were found to influence significantly the local strain distributions as well as the global stiffness of a tile-reinforced structure. Conventional shell-element-based analysis was examined to assess its limited ability to represent these essential deformation mechanisms. Two computationally efficient techniques were developed which represent the internal kinematics of a structure as accurately as a fully detailed three-dimensional analysis, while preserving a computational efficiency comparable to that of a shell-based analysis. These techniques are element layering and substructuring.

Element layering, like some advanced higher-order elements, predicts accurate global deformations by allowing the correct transverse shear deformations of the laminate to occur. One of the most important advantages of element layering over higher-order elements is that it is based on conventional finite elements. Element-layered models are portable from one analysis code to another, which is a prerequisite in a program that involves the computational facilities of several manufacturers and government laboratories. In addition, the method was implemented into an auto-layering program that automatically transforms any conventional shell model into an element-layered model.

Substructuring greatly reduces the computational cost of analyzing large components with either solid elements or element-layered superelements. Using pre-defined superelement libraries, it is straightforward to develop efficient models of large CAV-type structural components that can be analyzed rapidly on any typical desktop workstation.

References

1. Dávila, C.G., Smith, C. and Lumban-Tobing, F., 'Analysis of Thick Sandwich Shells with Embedded Ceramic Tiles', *Proc. 11th DoD/NASA/FAA Conference on Fibrous Composites in Structural Design* **1**, WL-TR-97-3008, Fort Worth, TX, August 1996.
2. Whitney, J. M., 'Shear Correction Factors for Orthotropic Laminates Under Static Load', *J. Applied Mechanics ASME* **40**, 1973, pp. 302-304.
3. Cho, Y-B. and Averill, R. C., 'An Improved Theory and Finite-Element Model for Laminated Composite and Sandwich Beams Using First-Order Zig-Zag Sublaminate Approximations', *Composite Structures* **37**(3-4), 1997, pp. 281.
4. Wang, J. T., Raju, I. S., Dávila, C. G. and Sleight, D. W, 'Computation of Strain Energy Release Rates for Skin-Stiffener Debonds Modeled with Plate Elements', *Proc. AIAA/ASME/ASCE/AHS 34th Structures, Structural Dynamics, and Materials Conference*, April 1993. AIAA Paper 93-1501.
5. Pike, T., Lumban-Tobing, F., Smith, C. and Garcia, R., 'Composite Armored Vehicle Component Analysis and Test Result Correlation,' *Proc. 11th DoD/NASA/FAA Conference on Fibrous Composites in Structural Design*, **1**, WL-TR-97-3008, Fort Worth, TX, 1996.

6. Anon., ABAQUS Theory Manual, Version 5.5, Hibbit Karlsson & Sorensen, Inc., Pawtucket, RI, 1995, pp. 2.13.1-2.
7. Anon., ABAQUS User's Manual, Version 5.6, Hibbit Karlsson & Sorensen, Inc. Pawtucket, RI, 1996.
8. Dávila, C. G., Baker, D. J. and Taylor, S., 'Superelement Analysis of Tile-Reinforced Composite Armor', *Report VTC NR 97-04*, Army Research Laboratory, NASA Langley Research Center, Hampton, VA, 1997.
9. Anon., MSC PATRAN V7.5 User's Manual, McNeal-Schwendler Corp., Los Angeles, CA, 1997.
10. Dávila, C. G., 'Superelement Analysis of Tile-Reinforced Composite Armor', *Proc. 11th Worldwide ABAQUS User's Conference*, Newport, RI, 1998.
11. Dávila, C. G., Chen, Tzi-Kang and Baker, D. J., 'Analysis of Tile-Reinforced Composite Armor. Part1: Advanced Modeling and Strength Analyses', *Proc. 21st Army Science Conference*, Norfolk, VA, 1998.

REPORT DOCUMENTATION PAGE

Form Approved
OMB No. 0704-0188

1. AGENCY USE ONLY (*Leave blank*)	2. REPORT DATE	3. REPORT TYPE AND DATES COVERED
	July 1999	Technical Memorandum

4. TITLE AND SUBTITLE
Advanced Modeling Strategies for the Analysis of Tile-Reinforced Composite Armor

5. FUNDING NUMBERS
538-13-12

6. AUTHOR(S)
Carlos G. Dávila and Tzi-Kang Chen

7. PERFORMING ORGANIZATION NAME(S) AND ADDRESS(ES)
NASA Langley Research Center
Hampton, VA 23681-2199

U.S. Army Research Laboratory
Vehicle Technology Directorate
NASA Langley Research Center
Hampton, VA 23681-2199

8. PERFORMING ORGANIZATION REPORT NUMBER
L-17850

9. SPONSORING/MONITORING AGENCY NAME(S) AND ADDRESS(ES)
National Aeronautics and Space Administration
Washington, DC 20546-0001
and
U.S. Army Research Laboratory
Adelphi, MD 20783-1145

10. SPONSORING/MONITORING AGENCY REPORT NUMBER
NASA/TM-1999-209352
ARL-TR-1978

11. SUPPLEMENTARY NOTES
POC/Phone: Carlos G. Dávila, 757-864-9130

12a. DISTRIBUTION/AVAILABILITY STATEMENT
Unclassified-Unlimited
Subject Category 39 Distribution: Nonstandard
Availability: NASA CASI (301) 621-0390

12b. DISTRIBUTION CODE

13. ABSTRACT (*Maximum 200 words*)
A detailed investigation of the deformation mechanisms in tile-reinforced armored components was conducted to develop the most efficient modeling strategies for the structural analysis of large components of the Composite Armored Vehicle. The limitations of conventional finite elements with respect to the analysis of tile-reinforced structures were examined, and two complementary optimal modeling strategies were developed. These strategies are element layering and the use of a tile-adhesive superelement. Element layering is a technique that uses stacks of shear deformable shell elements to obtain the proper transverse shear distributions through the thickness of the laminate. The tile-adhesive superelement consists of a statically condensed substructure model designed to take advantage of periodicity in tile placement patterns to eliminate numerical redundancies in the analysis. Both approaches can be used simultaneously to create unusually efficient models that accurately predict the global response by incorporating the correct local deformation mechanisms.

14. SUBJECT TERMS
composite armor, tile-reinforced sandwich structure, element layering, superelements

15. NUMBER OF PAGES
21

16. PRICE CODE
A03

17. SECURITY CLASSIFICATION OF REPORT	18. SECURITY CLASSIFICATION OF THIS PAGE	19. SECURITY CLASSIFICATION OF ABSTRACT	20. LIMITATION OF ABSTRACT
Unclassified	Unclassified	Unclassified	UL

NSN 7540-01-280-5500

Standard Form 298 (Rev. 2-89)
Prescribed by ANSI Std. Z-39-18
298-102